A comparative study on the in vitro biotransformation of medicagenic acid using human liver microsomes and S9 fractions

A comparative study on the *in vitro* biotransformation of medicagenic acid using human liver microsomes and S9 fractions

Laura PEETERS[1,†,*], Philippe VERVLIET[2,†], Kenn FOUBERT[1], Nina HERMANS[1], Luc PIETERS[1], Adrian COVACI[2,*]

[1] Natural Products & Food Research and Analysis (NatuRA), Department of Pharmaceutical Sciences, University of Antwerp, Universiteitsplein 1, 2610 Antwerp (Wilrijk), Belgium

[2] Toxicological Centre, Department of Pharmaceutical Sciences, University of Antwerp, Universiteitsplein 1, 2610 Antwerp (Wilrijk), Belgium

[†]: Joint first authors

*Corresponding authors: laura.peeters@uantwerpen.be, adrian.covaci@uantwerpen.be

Abstract

Many natural products are prodrugs which are biotransformed and activated after oral administration. The investigation of gastrointestinal and hepatic biotransformation can be facilitated by *in vitro* screening methods. This study compares two widely used *in vitro* models for hepatic biotransformation: 1) human S9 fractions and 2) human liver microsomes and cytosolic fractions in a two-step sequence, with the purpose of identifying differences in the biotransformation of medicagenic acid, the putative precursor of active metabolites, responsible for the medicinal effects of the herb *Herniaria hirsuta*. The combination of liquid chromatography coupled to high-resolution mass spectrometry with subsequent suspect and non-target data analysis allowed the identification of thirteen biotransformation products, four of which are reported here for the first time. Eight biotransformation products resulting from oxidative Phase I reactions were identified. Phase II conjugation reactions resulted in the formation of three glucuronidated and two sulfated biotransformation products.

No major differences could be observed between incubations with human liver S9 or when utilizing human microsomal and cytosolic fractions. Apart from two metabolites, both methods rendered the same qualitative metabolic profile, with minor quantitative differences. As a result, both protocols applied in this study can be used to study *in vitro* human liver biotransformation reactions.

Keywords: *In vitro* liver biotransformation, medicagenic acid, non-target screening, human liver microsomes, human liver S9

1. Introduction

Until today, the world faces several diseases for which no suitable treatment is available. One approach to find new remedies is the investigation of the active constituents of traditionally used herbal medicines, which in many cases are not known [1,2]. This is usually done by bioassay-guided isolation. However, bioassay-guided isolation is limited to the use of *in vitro* test systems, because many fractions and subfractions have to be tested, and large-scale *in vivo* testing comes up against practical and ethical constraints. Therefore, an important disadvantage of bioassay-guided fractionation is that many natural products, e.g. glycosides, are prodrugs which have to be biotransformed and activated after oral administration. Consequently, they are not detected in an *in vitro* test, but this aspect is usually overlooked when searching for new therapeutic agents using classical approaches [3]. Overlooking biotransformation might lead to unexpectedly low *in vitro* activity, compared to *in vivo* evidence or traditional use. A well-known example includes the metabolic activation of salicin from willow bark, which is deglycosylated by microbial fermentation in the colon, and oxidised to salicylic acid in the liver [4]. In addition, current guidelines encourage the use of *in vitro* screening before *in vivo* experiments to reduce, refine or replace the use of laboratory animals [5]. *In vitro* biotransformation comprises two main organ systems: gastrointestinal biotransformation and hepatic biotransformation.

In vitro hepatic biotransformation, including both Phase I and II biotransformation, can be assessed by different models, ranging from whole cell systems, including intact perfused liver and human hepatocytes cultures, to enzyme preparations, including liver microsomes, cytosolic and S9 fractions [6]. Each method has its own drawbacks and benefits. The choice of method is mainly determined by the research question. In the quest to reveal active constituents present in plant extracts, the goal is to disclose the biotransformation mechanism and to reveal which metabolites are formed. Therefore, the ease of application and affordability are important parameters for high throughput screening of compounds [6]. Based on these criteria, two *in vitro* hepatic biotransformation models were selected: 1) human S9 fractions and 2) human liver microsomes and cytosolic fractions in a two-step sequence . Literature states that S9 fractions offer a more complete representation of the metabolic profile compared to microsomes and cytosol, as they contain both Phase I and II enzymes [6]. One of the drawbacks of this method is lower enzyme activity in the S9 fraction compared to microsomes or cytosol, whereby some metabolites may be overlooked.

Therefore, the aim of this study was to compare the *in vitro* biotransformation using either human S9 fraction or using human liver microsomes and cytosol. For this purpose, medicagenic acid was selected as model compound. This triterpene is the major metabolite after *in vitro* gastrointestinal biotransformation of mono- or bidesmodic saponins (i.e. triterpene glycosides) present in the medicinal plant species *Herniaria hirsuta*, of which extracts are widely used against urinary stones and

as a diuretic [7]. After deglycosylation by the microflora in the colon, the aglycone is absorbed and is further biotransformed in the liver [8]. The gastrointestinal biotransformation has already been studied in a previous report, but the hepatic biotransformation has not been investigated yet and might give additional information on possible active metabolites of *Herniaria hirsuta* extracts [9].

2. Materials and methods

2.1. Chemicals and reagents

Ultrapure water with a resistivity of 18.2 MΩ.cm at 25 °C was generated with a Millipore™-purification system. UPLC-grade methanol and acetonitrile were purchased from Biosolve (France), dichloromethane was acquired from Merck (Germany). A standard mixture for quality control (QC) purposes was prepared including the following analytical standards: apigenin, benzoic acid, caffeic acid, catechin, chlorogenic acid, cinnamic acid, coumarin, emodin, epicatechin, ferulic acid, isorhamnetin, naringenin, p-coumaric acid, protocatechuic acid, quercetin, quercitrin, rutin, salicylic acid, sinapic acid, β-sitosterol, stigmasterol, syringic acid, tannic acid, taxifolin, theophylline, and vanillic acid (provided by Sigma Aldrich, USA); luteolin and procyanidin B2 (provided by Santa Cruz Biotechnology, USA); gallic acid and p-hydroxybenzoic acid (provided by Carl Roth, Belgium). The substrate medicagenic acid (purchased from Phytolab, Germany) was prepared in a mixture of DMSO:MeOH (20:80, v:v) to assure that DMSO was kept below 0.2% of total incubation mixture and methanol did not exceed 1% [10]. Human liver S9 fraction (mixed gender, n = 200, protein concentration = 20 mg mL^{-1}), HLM (mixed gender, n = 50, protein concentration = 20 mg mL^{-1}), HLCYT (mixed gender, n = 50, protein concentration = 20 mg mL^{-1}) and NADPH RS (Regenerating System) were purchased from Sekisui XenoTech (USA). All other chemicals and biochemicals were purchased from Sigma-Aldrich (USA).

2.2. Preparation of standard solutions

Standard stock solutions for the phenolic analytes were prepared at a concentration of 1 mg mL^{-1} in UPLC-grade methanol for each analyte separately and stored in the dark at 4 °C. Dilutions of these solutions were prepared in MeOH:H_2O + 40 mM ammonium formate buffer (60:40, v:v). Standard stock and working solutions were stored at −20 °C in the dark. QC samples were prepared using a dilution of the standard solution mix (39 ng mL^{-1}).

2.3. Liver biotransformation using S9

Liver biotransformation mimicking Phase I and II reactions of medicagenic acid was simulated *in vitro* by using pooled human S9 fractions. Samples were prepared in triplicate and consisted of a mixture of 65 mM TRIS buffer (pH adjusted to 7.4 at 37 °C), human liver S9 fraction (1 mg mL^{-1} final protein

concentration) and medicagenic acid (100 µM final concentration), prepared in a total volume of 0.5 mL and preincubated in a shaking water bath at 37 °C. The reaction was initiated by addition of a NADPH regenerating system (0.6 mM NADP, final concentration). Alamethicin (10 µg mL^{-1} final concentration in TRIS buffer) was added to the reaction mixture to increase permeability and to enhance Phase II glucuronidation reactions [11,12]. Co-factors were added after 5, 60 and 120 min to expose the samples to Phase II conjugation through glucuronidation and sulfation: UDPGA (2 mM final concentration), GSH (2 mM final concentration) and PAPS (0.1 mM final concentration). The reaction was inhibited after 1 h or 3 h by adding 0.5 mL of acetonitrile and storing the tubes on ice. Thereafter, the tubes were centrifuged for 5 min at 10000 rpm (4 °C). Then, the supernatant was collected and analyzed by LC-MS. Method blank (MB) samples were prepared as described above, but with solvent instead of substrate. Negative control (NC) samples were prepared in duplicate by leaving out S9 and cofactors and adding acetonitrile at 0, 1 or 3 h to quench the biotransformation reactions. A positive control was included by incubating testosterone (100 µM final concentration) [11].

2.4. Liver biotransformation using human liver microsomes and human liver cytosol

In vitro liver biotransformation of medicagenic acid using human HLM and HLCYT mimicking Phase I and II reactions respectively was simulated. Samples for phase I biotransformation were prepared in triplicate and consisted of a mixture of 65 mM TRIS buffer (pH adjusted to 7.4 at 37 °C), HLM (1 mg mL^{-1} final protein concentration) and medicagenic acid (100 µM final concentration) in a total volume of 0.5 mL and preincubated in a shaking water bath at 37 °C. The reaction was initiated by addition of NADPH RS (0.6 mM NADP, final concentration). The reaction was inhibited after 1 h or 3 h by adding 0.5 mL of acetonitrile and storing the tubes on ice. Thereafter, the tubes were centrifuged for 5 min at 10000 rpm (4 °C) and supernatant was collected.

Samples for Phase II biotransformation, also prepared in triplicate, underwent Phase I reactions as described above. After 3 h they were quenched on ice, centrifugated for 5 min at 10000 rpm (4 °C) and the supernatant was collected. To mimic glucuronidation, the supernatant obtained after Phase I was added to a mixture of 65 mM TRIS buffer (pH adjusted to 7.4 at 37 °C), fresh HLM (1 mg mL^{-1} final protein concentration), alamethicin (10 µg mL^{-1} final concentration) in a total volume of 0.47 mL. 10 µL of UDPGA (100 mM in TRIS-buffer) was added after 5, 60 and 120 min. The reaction was quenched after 3 h by adding 0.5 mL of acetonitrile and storing the tubes on ice. Samples where Phase I was simulated in combination with glucuronidation are referred to as HLM_Gluc.

To simulate sulfation and reactions including glutathion-S-transferase (HLM_Sulf), the supernatant obtained after Phase I was added to a mixture of 65 mM TRIS buffer (pH adjusted to 7.4 at 37 °C), HLCYT (1 mg mL^{-1} final protein concentration), alamethicin (10 µg mL^{-1} final concentration) in a total volume of 0.44 mL. After 5, 60 and 120 min, 10 µL of GSH (2 mM final concentration) and PAPS (0.1

mM final concentration) was added to the reaction mixture. Thereafter, the tubes were centrifuged for 5 min at 10000 rpm (4 °C). Then, the supernatant was collected and analyzed by LC-MS. Method blank samples were prepared as described above, but with solvent instead of substrate.

Negative control samples for Phase I were prepared by leaving out HLM and cofactors during Phase I and adding acetonitrile after 0, 1, or 3 h of incubation to quench the biotransformation reactions. A positive control for Phase I was included by incubating testosterone (100 µM final concentration). For Phase II, negative controls were prepared by leaving out the subcellular fraction and cofactors during the Phase II incubations, and a positive control was included by incubating 4-nitrophenol (4-NP) (10 µL of 10 mM in TRIS-buffer) and monitoring the formation of 4-NP glucuronide and 4-NP sulfate [11,13].

2.5. Instrumental Analysis

For the qualitative UPLC-DAD-QTOF analyses of the biotransformation samples, an aliquot of 5 µL was injected on Waters ACQUITY LC system equipped with MassLynx 4.1 software. Separation was achieved using a BEH-Shield-RP18 column (100 mm x 2.1 mm, 1.7 µm, Waters, Milford, MA, USA). The temperature of the column was kept at 40 °C. The mobile phase solvents consisted of water + 0.1% formic acid (A) and acetonitrile + 0.1% formic acid (B) and the gradient was set as follows (min/B%): 0/2, 1/2, 14/26, 24/65, 26/100, 29/100, 31/2, 41/2. The flow rate was set at 0.4 mL min^{-1}. For detection, accurate mass measurements were done using a Xevo G2-XS QTof spectrometer (Waters, Milford, MA, USA) coupled online to the LC-system. During the first analysis, full scan data were recorded in ESI (+) and ESI (-) mode from *m/z* 50 to 2000 in sensitivity mode (approximate resolution: 22000 FWHM). The spray voltage was set at either +1.5 kV and -1.0 kV; cone gas flow and desolvation gas flow at 50 L h^{-1} and 1000 L h^{-1} respectively; source temperature and desolvation temperature at 120 °C and 500 °C, respectively. Data were also recorded using MS^E in positive and negative ionization modes, and a ramp collision energy from 20 V to 30 V was applied. Leucine encephalin was used as lock mass. To monitor analytical drift and assess precision, QC samples were injected after series of samples of the same time point.

2.6. Data analysis

Suspect screening methods, involving *in silico* metabolite prediction, were combined with a non-target screening workflow to enhance the identification of products formed by *in vitro* liver biotransformation [13]. A list of potential biotransformation products was generated using Meteor Nexus 2.1 (Lhasa Limited, Leeds, UK). For Phase I biotransformation, all redox and non-redox biotransformation reactions were selected. For Phase II biotransformation, *O*-glucuronidation, *O*-sulfonylation, acetylation and conjugation with amino acids were selected. The maximum number of sequential biotransformations (depth) was set at 3, and the maximum number of biotransformation

products at 1000. Biotransformer was used as an additional software tool to predict Phase II metabolites. The tool combines a knowledge-based approach with a machine-learning-based approach to predict biotransformation [14]. The SMILES string of medicagenic acid was uploaded, and "Phase I Transformation" and "Phase II Transformation" options were selected separately. The generated csv file contained InChIKey, synonyms, major isotope mass, molecular formula, type of biotransformation reaction, and precursor ID. A complete list of *in silico* predicted biotransformation products can be found in Table SI 1.

In addition, a non-target screening workflow was performed starting by converting raw data files to mzXML data files to allow processing with XCMS (version 3.6.2) in R (version 3.6.1) [15-18]. Data from the different biotransformation experiments (S9, HLM_Gluc and HLM_Sulf) were treated separately. The XCMS CentWave algorithm was used to pick features from the raw data, followed by a grouping step, a retention time alignment over the different samples and re-iterative filling of missing peaks. Details on the parameters for these algorithms can be found in the Supporting Information.

To compare between groups (sample, method blank and negative control), taking the longitudinal aspect into account, resulting features were further analyzed in R using the edge package [19,20]. A set of training data was selected based on low p-values (<0.0001) from the two EDGE-analyses (sample vs. method blank and sample vs. negative control) resulting in 796, 658 and 936 MS time profiles for S9, HLM_Gluc and HLM_Sulf respectively. Tinderesting, an interactive Shiny app developed in R, was used to rate the quality of the resulting time profiles of these features to train a random forest model for predicting experts response [21]. The machine learning model provided a single score for each feature, referred to as tinderesting score, which allowed ranking of all features based on the difference over time between the three groups. The maximal score of 1 corresponds to the model labelling this feature as interesting, and the minimal score of 0 defines an uninteresting feature. The machine learning model ranked 5794 features for S9, 6709 for HLM_Gluc, and 6202 for HLM_Sulf.

Features which were marked as interesting by the machine learning model were further filtered based on their fold change between samples and negative controls. A volcano plot was constructed to plot the *p*-value from a student t-test as a function of the calculated fold change for every feature with a retention time > 2 min. Features with a *p*-value lower than 0.05 and a fold change higher than 10 were selected for in depth investigation [22]. This filtering step reduced the number of features for the different groups to 140 for S9, 52 for HLM_Gluc, and 82 for HLM_Sulf.

Facet plots were constructed in R displaying on overlay of the extracted ion chromatograms (EIC) of the replicates for the different sample types (sample, negative control and method blank) separately for each group (S9, HLM_Gluc, and HLM_Sulf). The progression of the intensity over time was visually evaluated, including evaluation of the similarity in peak shape and area for different replicates of the

same sample type. To assure that only metabolites are included after hepatic biotransformation, biotransformation products were only included if they are not present in the blank and negative control samples, while they are present in all replicates of the sample at the same retention time. A list of 180 features in total remained and isotopes and adducts were filtered out manually. As a last step, boxplots were generated to compare the intensity of the feature between the different groups over time, allowing a semi-quantitative comparison of metabolite formation.

To have a qualitative overview of metabolites, tentative identification of the resulting biotransformation products was based on the accurate mass, isotopic pattern and fragmentation pattern of the product ions. A maximal mass variation between theoretical and observed was set at 10 ppm for parent ions and 25 ppm for product ions. Molecular formulas of the resulting metabolites were predicted by the Elemental Composition algorithm in MassLynx software based on the observed *m/z* values.

The relative abundances of the tentatively identified metabolites were compared to the abundance of the parent compound before biotransformation to assess quantitative differences between metabolite formation after hepatic biotransformation using the S9 fractions versus using HLM + HLCYT.

3. Results and discussion

Incubating medicagenic acid with human liver S9 fractions or HLM for 3 h resulted in the clearance of 14% and 18% of the parent compound, respectively (Figure 1). Along with the decrease in intensity of the signal for medicagenic acid, formation of metabolites was observed with an increase in intensity of their signal over time. This was confirmed by differences observed in the total ion chromatograms (TIC), before, during and after hepatic biotransformation (Figure SI 1 and Figure SI 2). To have a first impression of the differences between both *in vitro* biotransformation methods, suspect screening was performed, using the *in silico* predictions of Meteor and Biotransformer. Thereafter, a non-target screening method was used to tentatively identify new metabolites.

3.1. Suspect screening

Suspect screening analysis resulted in detection of several metabolites summarized in Table 1. Figure 2 shows an overview of the proposed metabolic pathway of medicagenic acid after *in vitro* hepatic biotransformation. For metabolites 1-3 (**M1-3**) (*m/z* 517.3165 $[M-H]^-$), three chromatographically separated peaks were observed, suggesting the presence of three different structural isomers. This was confirmed by the prediction provided by Meteor which predicted hydroxylation (+16 from the parent) at C-11, C-24, or C-29. Double hydroxylation (+32 from the parent) (**M4**) (*m/z* 533.3114 $[M-H]^-$), oxidation of a hydroxyl group (-2 from the parent) (**M5**) (*m/z* 499.3060 $[M-H]^-$) and a combination of hydroxylation and oxidation (+30 from the parent) (**M6-7**) (*m/z* 531.2958 $[M-H]^-$), were also predicted

by Meteor. The major Phase II products observed were glucuronidated metabolites of medicagenic acid (**M8-9**) (*m/z* 677.3537 $[M-H]^-$). However, the poor MS/MS fragmentation of medicagenic acid and the lack of NMR data rendered the identification as tentative. Further elucidation of the molecular structures was not possible.

Despite prediction of sulfation reactions of medicagenic acid by Meteor and Biotransformer, sulfated conjugates were not observed in the biotransformation experiments. To confirm that the *in vitro* model was capable to form sulfated conjugates, the biotransformation of testosterone was examined as positive control. Testosterone metabolites were detected after hepatic biotransformation and proved the capability of the *in vitro* model to form both sulfated and glucuronidated conjugates (Figure SI 3).

3.2. Non-target screening

For each biotransformation experiment (S9, HLM_Gluc and HLM_Sulf), a random forest model was trained based on selected time profiles. The area's under the curves (AUC) of receiver operator characteristic (ROC) curves were 0.999, 0.978 and 0.996 for S9, HLM_Gluc and HLM_Sulf, respectively (Figure SI 4). The applied non-target screening analysis was capable of picking up all features also discovered by the suspect screening approach, confirming its applicability to discover biotransformation products. In total, 4 additional biotransformation products could be identified using the non-target screening approach.

First, a hitherto unknown compound with *m/z* 597.2689 $[M-H]^-$ was identified at a retention time of 18.82 min (**M10**). Figure 3 displays the MS^2 spectrum, showing a product ion at *m/z* 501.3130 $[M-H]^-$, suggesting that the compound is a metabolite of medicagenic acid. The ion at *m/z* 515.2997 $[M-H]^-$ originates from medicagenic acid substituted with an additional hydroxyl group and loss of H_2. Combining the limited fragmentation information with the *m/z* 597.2715 $[M-H]^-$ supports a molecular formula of $C_{30}H_{46}O_{10}S$ suggesting hydroxylation followed by sulfation. This metabolite is only observed after 3 h of *in vitro* hepatic biotransformation, suggesting further Phase 2 biotransformation of **M1-3.** Figure 4 shows a bar graph comparing the difference in abundance of **M10** between the different sample groups at different time points. A structural isomer was observed in the samples combining HLM with HLCYT at a retention time of 19.85 min (**M11**).

Figure 5 and Figure SI 6 show the relative abundance of **M10** and **M11** over time. An increase in intensity is observed over time, which is not observed in the negative control samples (NC) and the method blank (MB).

Given the absence of specific MS/MS product ions when fragmenting medicagenic acid and any of its metabolites, screening with LC-MS does not allow full structural elucidation. Therefore, isomers such as **M1/M2/M3** and **M10/M11** can only be separated based on retention time without further information on the linkage position.

In addition to **M10-11,** the non-target screening approach resulted in the tentative identification of two additional metabolites (**M12** and **M13**)**. M12** is an oxidated metabolite (*m/z* 515.3009 $[M-H]^-$) and is observed in S9 and HLM_Sulf. **M13**, a metabolite showing hydroxylation followed by glucuronidation (*m/z* 693.3486 $[M-H]^-$) was only observed after simulation of hepatic biotransformation using S9. As **M13** is a two-step biotransformation product only observed in the last sampling point, it most probably originates from **M1-3.** Table 1 shows an overview of all tentatively identified metabolites.

According to Jing et al., sulfated and glucuronidated conjugates can serve as substrates for further biotransformation. They describe both initial sulfation and subsequent glucuronidation, or alternatively initial glucuronidation followed by further sulfation of glycyrrhetic acid (GA). However, this two-step Phase II biotransformation pathway is not observed for medicagenic acid [23].
The non-target screening approach confirmed the formation of the predicted metabolites and rendered four additional metabolites. However, limited by the poor MS/MS fragmentation of the aglycones and lack of NMR data, identification remains tentative.

3.3. S9 vs HLM biotransformation

Table 1 shows the relative abundance of the metabolites. Combination of microsomal and cytosolic fractions is necessary to allow both glucuronidation and sulfation reactions, resulting in a similar qualitative profile of metabolites obtained after biotransformation using S9 fractions. This is partly in accordance to earlier work by Van Den Eede *et al,* who investigated the biotransformation of flame retardants and plasticizers using HLM and S9 [11]. They reported that all Phase I metabolites of HLM-incubations could also be identified in incubations with S9 fractions, albeit at lower concentrations. In our results, we could only identify quantitative differences for hydroxylated metabolites **(M1-3)**. While **M1** and **M2** were more abundant when using microsomal and cytosolic fractions, metabolite **M3** had a higher relative abundance in the S9 incubations. For the other metabolites, the relative abundance was similar between both *in vitro* methods. Based on their results, Van Den Eede *et al* suggested that quantitative differences for substrate and metabolites between HLM and S9 fractions could be explained by a higher concentration of CYP-enzymes in HLM than in S9 per unit of total protein content [11,24]. These differences are not as pronounced for medicagenic acid and its biotransformation products, suggesting different behaviour for specific chemical classes.

In this study, only small differences in the metabolic profile were observed between the different incubation experiments using S9 and microsomal and cytosolic fractions. This was in accordance with previous work by Jaeg *et al*, who could not observe major differences in biotransformation of bisphenol A when using either mouse liver microsomes or S9 fractions and Dalvie *et al* who compared biotransformation reactions between hepatocytes, S9-fractions and HLM for different pharmaceuticals [25,26]. In the present study, only two differences could be found in the identification of biotransformation products of medicagenic acid. Metabolite **M13** was only observed after S9 biotransformation and was not detected when microsomal and cytosolic fractions were used. Formation of this biotransformation product requires Phase I hydroxylation and subsequent Phase II glucuronidation. These reactions are combined using S9 fractions, while they are performed separately when using the two-step biotransformation assay. Combination of Phase I and II reactions might lead to a more complete biotransformation profile, favouring the use of S9 fractions. On the other hand, **M11,** the structural isomer of **M10,** was only observed when using microsomal and cytosolic fractions. The lower enzyme activity of S9 fractions compared to the two-step biotransformation assay might prevent formation or detection of this isomer and is one of the drawbacks of biotransformation with S9 fractions [6].

Since metabolite profiles after biotransformation with either of the applied models are comparable in terms of qualitative and quantitative abundance, both hepatic biotransformation models are suitable for *in vitro* metabolite prediction. However, this comparison only included medicagenic acid. To draw general conclusions, other classes of chemical compounds should be included as well.

4. Conclusions

In vitro hepatic biotransformation reducing *in vivo* experiments requires a reliable *in vitro* screening method. Medicagenic acid was subjected to two widely used *in vitro* models simulating hepatic biotransformation: 1) human S9 fractions and 2) human liver microsomes for phase I biotransformations followed by a secondary incubation with either microsomal or cytosolic fractions for phase II conjugations. The results of a suspect screening method combined with non-target screening indicated formation of thirteen metabolites, of which four have never been reported before. Apart from two metabolites, both methods rendered the same qualitative metabolic profile, with minor quantitative differences. Despite the main reported disadvantage of S9 fractions having lower enzyme activity compared to HLM and HLCYT [6], the qualitative metabolite profile was similar, suggesting that the lower enzyme activity did not hamper detection of metabolites using LC-MS in the given experimental conditions. On the other hand, S9 fractions are able to combine Phase I and II

activity, reducing costs and time of analysis making this method favourable for the suggested metabolomics approach for rapid *in vitro* screening.

Acknowledgements

This study acknowledges the provision of funding through a Research Foundation Flanders (FWO) project (G089016N) and the Special Fund for Research of the University of Antwerp (Concerted Action), project ID no. 30732.

Conflicts of interest

The authors declare they have no conflict of interest.

References

1. Koehn, F.E.; Carter, G.T. Rediscovering natural products as a source of new drugs. *Discovery medicine* **2009**, *5*, 159-164.
2. Organization, W.H. General Guidelines for Methodologies on Research and Evaluation of Traditional Medicine. Availabe online: (accessed on 12/01/2020).
3. Liu, J.-H.; Yu, B.-Y. Biotransformation of bioactive natural products for pharmaceutical lead compounds. *Current organic chemistry* **2010**, *14*, 1400-1406.
4. Butterweck, V.; Nahrstedt, A. What Is the Best Strategy for Preclinical Testing of Botanicals? A Critical Perspective. *Planta Med* **2012**, *78*, 747-754, doi:10.1055/s-0031-1298434.
5. Ekins, S.; Ring, B.J.; Grace, J.; McRobie-Belle, D.J.; Wrighton, S.A. Present and future in vitro approaches for drug metabolism. *Journal of Pharmacological and Toxicological Methods* **2000**, *44*, 313-324, doi:https://doi.org/10.1016/S1056-8719(00)00110-6.
6. Fasinu, P.; J Bouic, P.; Rosenkranz, B. Liver-based in vitro technologies for drug biotransformation studies-a review. *Current drug metabolism* **2012**, *13*, 215-224.
7. Fouada, A.; Yamina, S.; Nait, M.A.; Mohammed, B.; Abdlekrim, R. In vitro and in vivo antilithiasic effect of saponin rich fraction isolated from herniaria hirsuta. *J Bras Nefrol* **2006**, *28*, 199-203.2006.
8. Osbourn, A.E. Preformed antimicrobial compounds and plant defense against fungal attack. *The plant cell* **1996**, *8*, 1821.
9. Peeters, L.; Van der Auwera, A.; Beirnaert, C.; Bijttebier, S.; Laukens, K.; Pieters, L.; Hermans, N.; Foubert, K. Compound Characterization and Metabolic Profile Elucidation after In Vitro Gastrointestinal and Hepatic Biotransformation of an Herniaria hirsuta Extract Using Unbiased Dynamic Metabolomic Data Analysis. *Metabolites* **2020**, *10*, 111.
10. Jia, L.; Liu, X. The conduct of drug metabolism studies considered good practice (II): in vitro experiments. *Current drug metabolism* **2007**, *8*, 822-829.
11. Van den Eede, N.; Maho, W.; Erratico, C.; Neels, H.; Covaci, A. First insights in the metabolism of phosphate flame retardants and plasticizers using human liver fractions. *Toxicology letters* **2013**, *223*, 9-15.
12. Fisher, M.B.; Campanale, K.; Ackermann, B.L.; VandenBranden, M.; Wrighton, S.A. In vitro glucuronidation using human liver microsomes and the pore-forming peptide alamethicin. *Drug metabolism and disposition* **2000**, *28*, 560-566.
13. Vervliet, P.; Van Den Plas, J.; De Nys, S.; Duca, R.C.; Boonen, I.; Elskens, M.; Van Landuyt, K.L.; Covaci, A. Investigating the in vitro metabolism of the dental resin monomers BisGMA, BisPMA, TCD-DI-HEA and UDMA using human liver microsomes and quadrupole time of flight mass spectrometry. *Toxicology* **2019**, *420*, 1-10.
14. Djoumbou-Feunang, Y.; Fiamoncini, J.; Gil-de-la-Fuente, A.; Greiner, R.; Manach, C.; Wishart, D.S. BioTransformer: a comprehensive computational tool for small molecule metabolism prediction and metabolite identification. *Journal of cheminformatics* **2019**, *11*, 1-25.
15. Stanstrup, J.; Gerlich, M.; Dragsted, L.O.; Neumann, S. Metabolite profiling and beyond: approaches for the rapid processing and annotation of human blood serum mass spectrometry data. *Analytical and bioanalytical chemistry* **2013**, *405*, 5037-5048.
16. Smith, C.A.; Want, E.J.; O'Maille, G.; Abagyan, R.; Siuzdak, G. XCMS: processing mass spectrometry data for metabolite profiling using nonlinear peak alignment, matching, and identification. *Analytical chemistry* **2006**, *78*, 779-787.
17. Tautenhahn, R.; Boettcher, C.; Neumann, S. Highly sensitive feature detection for high resolution LC/MS. *BMC bioinformatics* **2008**, *9*, 504.
18. Benton, H.P.; Want, E.J.; Ebbels, T.M. Correction of mass calibration gaps in liquid chromatography–mass spectrometry metabolomics data. *Bioinformatics* **2010**, *26*, 2488-2489.
19. Storey, J.; Leek, J.; Bass, A. edge: Extraction of Differential Gene Expression. R package version 2.0. 0. 2015.

20. Peeters, L.; Beirnaert, C.; Van der Auwera, A.; Bijttebier, S.; De Bruyne, T.; Laukens, K.; Pieters, L.; Hermans, N.; Foubert, K. Revelation of the metabolic pathway of Hederacoside C using an innovative data analysis strategy for dynamic multiclass biotransformation experiments. *Journal of Chromatography A* **2019**, *1595*, 240-247.
21. Beirnaert, C.; Peeters, L.; Meysman, P.; Bittremieux, W.; Foubert, K.; Custers, D.; Van der Auwera, A.; Cuykx, M.; Pieters, L.; Covaci, A. Using expert driven machine learning to enhance dynamic metabolomics data analysis. *Metabolites* **2019**, *9*, 54.
22. Vervliet, P.; Mortelé, O.; Gys, C.; Degreef, M.; Lanckmans, K.; Maudens, K.; Covaci, A.; van Nuijs, A.L.; Lai, F.Y. Suspect and non-target screening workflows to investigate the in vitro and in vivo metabolism of the synthetic cannabinoid 5Cl-THJ-018. *Drug testing and analysis* **2019**, *11*, 479-491.
23. Jing, J.; Ren, W.; Chen, X.; Wang, Y.; Yu, Q.; Wang, G.; Davey, A.K.; Wang, J.; Jing, N. Glucuronide-sulfate diconjugate as a novel metabolite of glycyrrhetic acid in rat bile. *Drug metabolism and pharmacokinetics* **2008**, *23*, 175-180.
24. Testa, B.; Krämer, S.-D. *The biochemistry of drug metabolism. 1, Principles, redox reactions, hydrolyses*; Helvetica Chimica Acta Wiley-VCH: 2008.
25. Jaeg, J.P.; Perdu, E.; Dolo, L.; Debrauwer, L.; Cravedi, J.-P.; Zalko, D. Characterization of new bisphenol A metabolites produced by CD1 mice liver microsomes and S9 fractions. *Journal of agricultural and food chemistry* **2004**, *52*, 4935-4942.
26. Dalvie, D.; Obach, R.S.; Kang, P.; Prakash, C.; Loi, C.-M.; Hurst, S.; Nedderman, A.; Goulet, L.; Smith, E.; Bu, H.-Z. Assessment of three human in vitro systems in the generation of major human excretory and circulating metabolites. *Chemical research in toxicology* **2009**, *22*, 357-368.

435 **Tables and figures**

436

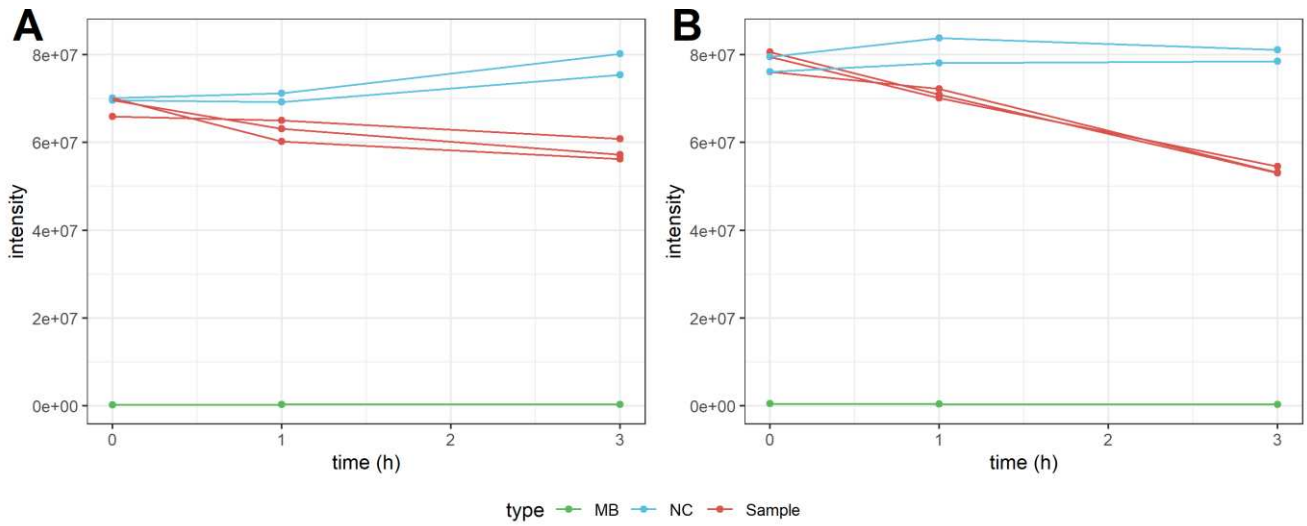

437

438 *Figure 1: Time profile of medicagenic acid in case of incubations with S9 (A) and HLM (B).*

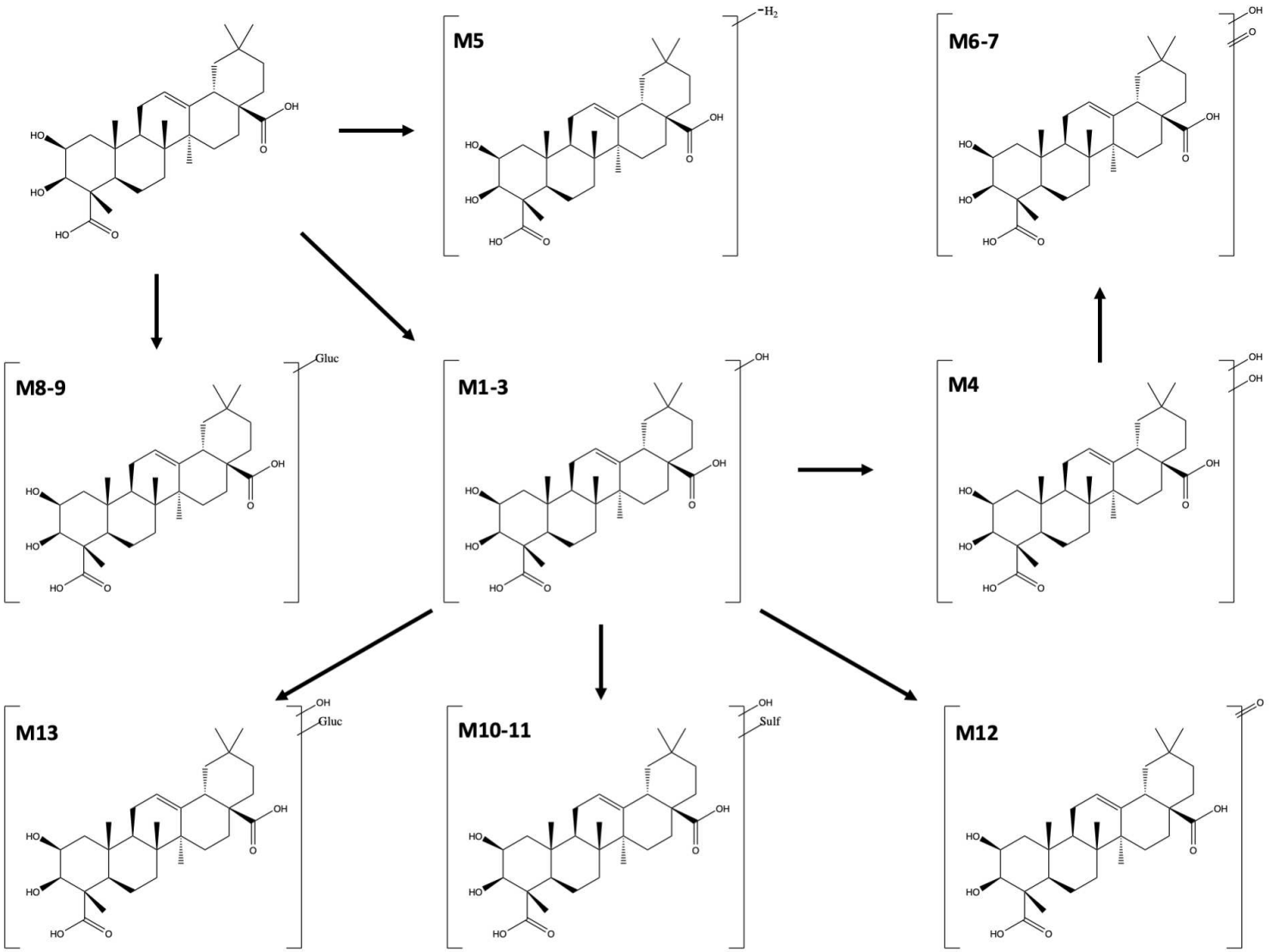

Figure 2: Suggested in vitro hepatic biotransformation pathway of medicagenic acid. Structural changes due to biotranformation reactions are represented with OH (hydroxylation), =O (hydroxylation and subsequent oxidation to keton), -H_2 (oxidation to keton), Gluc (conjugation with glucuronic acid) or Sulf (conjugation with sulfate).

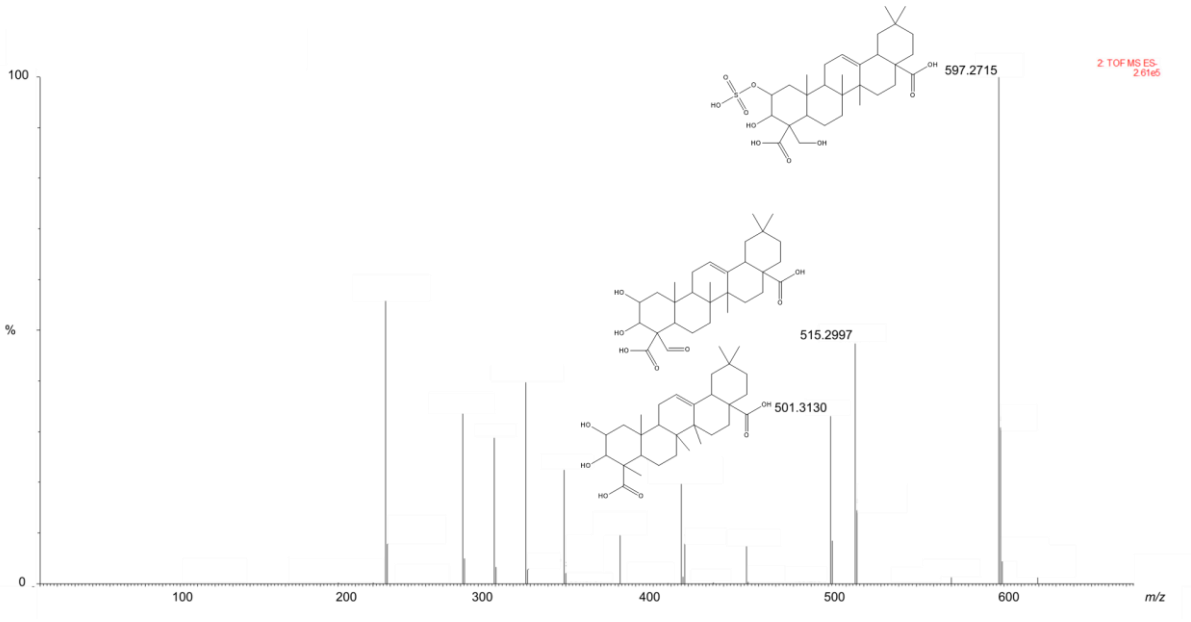

442

443 *Figure 3: MS² spectrum for m/z 597.2715*

444

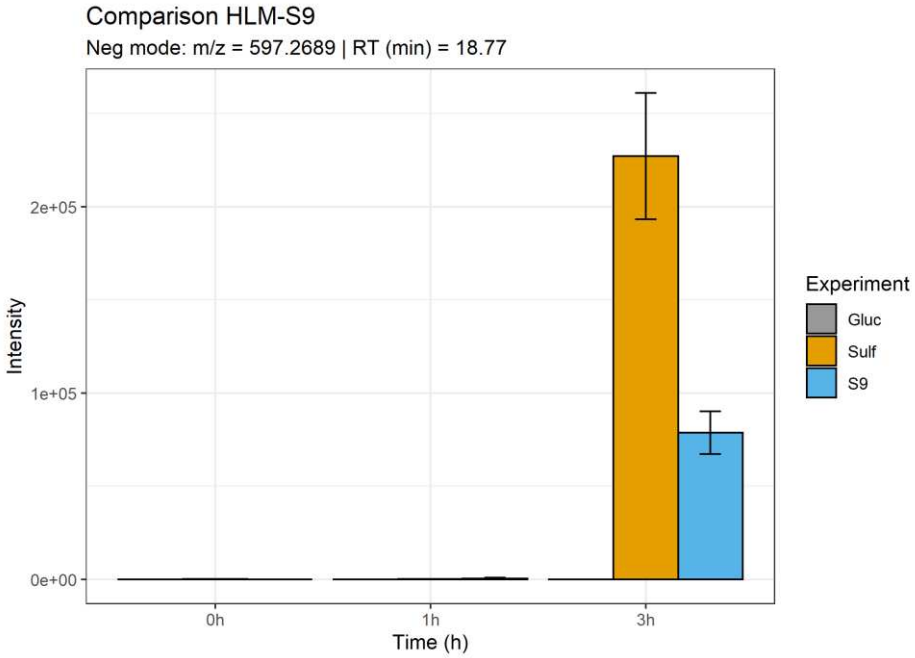

445

446 *Figure 4: Bar chart comparing the intensity for m/z 597.2689 [M-H] at retention time 18.77 min for the different samples*

447

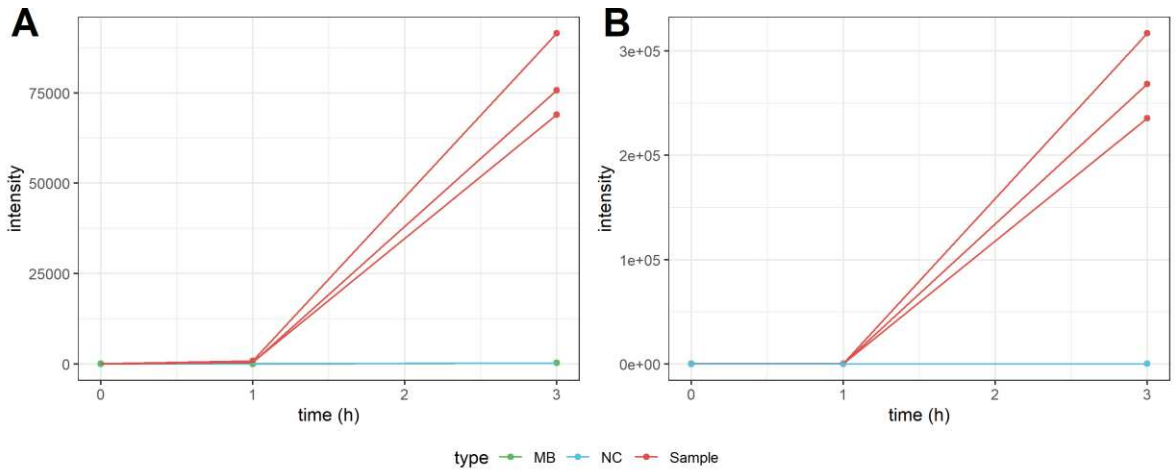

*Figure 5: Time profile of the biotransformation process for **M10** using S9 (A) and microsomal and cytosolic fractions (B) in samples, negative controls (NC) and blank (MB).*

451 *Table 1: Relative abundance of medicagenic acid and identified biotransformation products per incubation type.*

Name	*m/z* (observed)	RT (min)	Formula	Mass error (ppm)	MS/MS product ions	S9			HLM + HLCYT				
						0h	1h	3h	0h	1h	3h	Gluc	Sulf
MA	501.3216	21.70	$C_{30}H_{46}O_6$	0.0	483.3123 $[C_{30}H_{43}O_5]^-$	100	91.8	86.1	100	87.8	85.1	82.4	83.0
M1	517.3169	17.39	$C_{30}H_{46}O_7$	0.8	499.3056 $[C_{30}H_{43}O_6]^-$; 481.2972 $[C_{30}H_{41}O_5]^-$	0.0	2.0	4.4	0.0	11.3	16.1	23.1	17.3
M2	517.3166	17.60	$C_{30}H_{46}O_7$	0.2	499.3073 $[C_{30}H_{43}O_6]^-$; 481.3042 $[C_{30}H_{41}O_5]^-$	0.0	2.7	5.8	0.0	13.1	18.6	27.4	20.9
M3	517.3165	18.45	$C_{30}H_{46}O_7$	-1.9	501.3212 $[C_{30}H_{45}O_6]^-$; 499.3057 $[C_{30}H_{43}O_6]^-$	0.0	8.2	19.4	0.0	0.0	0.0	0.0	7.5
M4	533.3116	18.59	$C_{30}H_{46}O_8$	0.4	517.3159 $[C_{30}H_{45}O_7]^-$; 501.3215 $[C_{30}H_{45}O_6]^-$; 499.3045 $[C_{30}H_{43}O_6]^-$	0.0	1.3	3.1	0.0	0.0	0.0	0.0	2.3
M5	499.3060	20.71	$C_{30}H_{44}O_6$	0.0	481.2951 $[C_{30}H_{41}O_5]^-$	0.0	0.0	9.1	17.5	0.0	0.0	0.0	5.6
M6	531.2950	16.40	$C_{30}H_{44}O_8$	-1.5	515.2979 $[C_{30}H_{43}O_7]^-$	0.0	0.5	0.7	0.0	0.0	0.0	0.3	0.3
M7	531.2942	19.38	$C_{30}H_{44}O_8$	-3.0	515.3006 $[C_{30}H_{43}O_7]^-$; 499.3041 $[C_{30}H_{43}O_6]^-$	0.0	0.0	0.4	0.0	0.0	0.0	0.0	0.9
M8	677.3515	18.39	$C_{36}H_{44}O_{12}$	-3.2	517.3157 $[C_{30}H_{45}O_7]^-$; 501.3207 $[C_{30}H_{45}O_6]^-$; 499.3050 $[C_{30}H_{43}O_6]^-$	0.0	3.2	11.5	0.0	0.0	0.0	12.2	0
M9	677.3511	19.59	$C_{36}H_{44}O_{12}$	-3.8	501.3224 $[C_{30}H_{45}O_6]^-$; 483.3094 $[C_{30}H_{43}O_5]^-$	0.0	0.1	0.4	0.0	0.0	0.0	0.5	0.0
M10	597.2704	18.82	$C_{30}H_{46}SO_{10}$	-4.9	533.3117 $[C_{30}H_{45}O_8]^-$; 515.3007 $[C_{30}H_{43}O_7]^-$; 501.3187 $[C_{30}H_{45}O_6]^-$; 499.3018 $[C_{30}H_{43}O_6]^-$	0.0	0.0	0.2	0.0	0.0	0.0	0.0	0.7
M11	597.2718	19.85	$C_{30}H_{46}SO_{10}$	-2.5	517.3074 $[C_{30}H_{45}O_7]^-$; 515.3069 $[C_{30}H_{43}O_7]^-$; 499.3066 $[C_{30}H_{43}O_6]^-$	0.0	0.0	0.0	0.0	0.0	0.0	0.0	0.4
M12	515.3011	19.12	$C_{30}H_{44}O_7$	0.4	499.3029 $[C_{30}H_{43}O_6]^-$; 483.3078 $[C_{30}H_{43}O_5]^-$	0.6	19.2	29.4	0.3	0.6	0.7	0.0	19.7
M13	693.3467	15.36	$C_{36}H_{54}O_{13}$	-2.7	531.2964 $[C_{30}H_{43}O_8]^-$; 517.3131 $[C_{30}H_{45}O_7]^-$; 499.3029 $[C_{30}H_{43}O_6]^-$	0.0	0.0	0.3	0.0	0.0	0.0	0.0	0.0

452

SUPPORTING INFORMATION

A comparative study on the *in vitro* biotransformation of medicagenic acid using human liver microsomes and S9 fractions

Laura PEETERS[1,†,*], Philippe VERVLIET[2,†], Kenn FOUBERT[1], Nina HERMANS[1], Luc PIETERS[1], Adrian COVACI[2,*]

[1] Natural Products & Food Research and Analysis (NatuRA), Department of Pharmaceutical Sciences, University of Antwerp, Universiteitsplein 1, 2610 Antwerp, Belgium

[2] Toxicological Centre, Department of Pharmaceutical Sciences, University of Antwerp, Universiteitsplein 1, 2610 Antwerp, Belgium

[†]: Joint first authors

*Corresponding authors: laura.peeters@uantwerpen.be, adrian.covaci@uantwerpen.be

XCMS parameters

Peak picking:

CentWavePredIsoParam(ppm = 10, peakwidth = peak_width, snthresh = 10, noise = 1000, mzdiff = 0.01, prefilter = c(3,5000), integrate = 1)

Grouping:

PeakDensityParam(sampleGroups = rep(1, length(fileNames(res))), bw = 10, minFraction = 0.10, minSamples = 2, maxFeatures = 100, binSize = 0.015)

RT adjustment:

PeakGroupsParam(minFraction = 1, smooth = "loess", span = 0.6)

Tables and Figures

Table SI 1: In silico predictions of metabolites of medicagenic acid by Meteor and Biotransformer

	Formula	Exact Mass	Parent Formula	Reaction	InChi
Meteor	$C_{30}H_{46}O_7$	518.3244	$C_{30}H_{46}O_6$	Hydroxylation of aliphatic methyl carbon	InChI=1S/C30H46O7/c1-25(2)10-12-29(23(34)35)13-11-27(4)17(18(29)14-25)6-7-20-26(3)15-19(32)22(33)30(16-31,24(36)37)21(26)8-9-28(20,27)5/h6,18-22,31-33H,7-16H2,1-5H3,(H,34,35)(H,36,37)
	$C_{30}H_{44}O_8$	532.3036	$C_{30}H_{46}O_7$	Oxidation of primary alcohol	InChI=1S/C30H44O8/c1-25(2)10-12-29(22(33)34)13-11-27(4)16(17(29)14-25)6-7-19-26(3)15-18(31)21(32)30(23(35)36,24(37)38)20(26)8-9-28(19,27)5/h6,17-21,31-32H,7-15H2,1-5H3,(H,33,34)(H,35,36)(H,37,38)
	$C_{30}H_{46}O_8$	534.3193	$C_{30}H_{46}O_7$	Alkyl-OH hydroxylation	InChI=1S/C30H46O8/c1-25(2)8-10-29(23(35)36)11-9-27(4)16(17(29)13-25)12-18(32)21-26(3)14-19(33)22(34)30(15-31,24(37)38)20(26)6-7-28(21,27)5/h12,17-22,31-34H,6-11,13-15H2,1-5H3,(H,35,36)(H,37,38)
	$C_{30}H_{46}O_7$	518.3244	$C_{30}H_{46}O_6$	Alkyl-OH hydroxylation	InChI=1S/C30H46O7/c1-25(2)9-11-30(24(36)37)12-10-27(4)16(17(30)14-25)13-18(31)21-26(3)15-19(32)22(33)29(6,23(34)35)20(26)7-8-28(21,27)5/h13,17-22,31-33H,7-12,14-15H2,1-6H3,(H,34,35)(H,36,37)
	$C_{30}H_{46}O_8$	534.3193	$C_{30}H_{46}O_7$	Hydroxylation of aliphatic methyl carbon	InChI=1S/C30H46O8/c1-25(2)8-10-29(23(35)36)11-9-27(4)16(17(29)13-25)12-18(32)21-26(3)14-19(33)22(34)30(15-31,24(37)38)20(26)6-7-28(21,27)5/h12,17-22,31-34H,6-11,13-15H2,1-5H3,(H,35,36)(H,37,38)
	$C_{36}H_{54}O_{12}$	678.3615	$C_{30}H_{46}O_6$	*O*-glucuronidation of aliphatic acid	InChI=1S/C36H54O12/c1-31(2)11-13-36(30(46)48-28-24(40)22(38)23(39)25(47-28)27(42)43)14-12-33(4)17(18(36)15-31)7-8-20-32(3)16-19(37)26(41)35(6,29(44)45)21(32)9-10-34(20,33)5/h7,18-26,28,37-41H,8-16H2,1-6H3,(H,42,43)(H,44,45)
	$C_{36}H_{54}O_{12}$	678.3615	$C_{30}H_{46}O_6$	*O*-glucuronidation of aliphatic acid	InChI=1S/C36H54O12/c1-31(2)11-13-36(29(44)45)14-12-33(4)17(18(36)15-31)7-8-20-32(3)16-19(37)26(41)35(6,21(32)9-10-34(20,33)5)30(46)48-28-24(40)22(38)23(39)25(47-28)27(42)43/h7,18-26,28,37-41H,8-16H2,1-6H3,(H,42,43)(H,44,45)
	$C_{30}H_{46}O_7$	518.3244	$C_{30}H_{46}O_6$	Hydroxylation of aliphatic methyl carbon	InChI=1S/C30H46O7/c1-25(16-31)10-12-30(24(36)37)13-11-27(3)17(18(30)14-25)6-7-20-26(2)15-19(32)22(33)29(5,23(34)35)21(26)8-9-28(20,27)4/h6,18-22,31-33H,7-16H2,1-5H3,(H,34,35)(H,36,37)
	$C_{30}H_{44}O_6$	500.3138	$C_{30}H_{46}O_6$	Oxidation of secondary alcohol	InChI=1S/C30H44O6/c1-25(2)11-13-30(24(35)36)14-12-27(4)17(18(30)15-25)7-8-20-26(3)16-19(31)22(32)29(6,23(33)34)21(26)9-10-28(20,27)5/h7,18,20-22,32H,8-16H2,1-6H3,(H,33,34)(H,35,36)
Biotransformer	$C_{36}H_{54}O_{12}$	678.3615	$C_{30}H_{46}O_6$	Alkyl-OH glucuronidation	InChI=1S/C36H54O12/c1-31(2)11-13-36(30(45)46)14-12-33(4)17(18(36)15-31)7-8-20-32(3)16-19(47-28-24(39)22(37)23(38)25(48-28)27(41)42)26(40)35(6,29(43)44)21(32)9-10-34(20,33)5/h7,18-26,28,37-40H,8-16H2,1-6H3,(H,41,42)(H,43,44)(H,45,46)/t18-,19-,20+,21+,22?,23?,24?,25?,26-,28?,32+,33+,34+,35-,36-/m0/s1
	$C_{36}H_{54}O_{12}$	678.3615	$C_{30}H_{46}O_6$	Alkyl-OH glucuronidation	InChI=1S/C36H54O12/c1-31(2)11-13-36(30(45)46)14-12-33(4)17(18(36)15-31)7-8-20-32(3)16-19(37)26(35(6,29(43)44)21(32)9-10-34(20,33)5)48-28-24(40)22(38)23(39)25(47-28)27(41)42/h7,18-26,28,37-40H,8-16H2,1-6H3,(H,41,42)(H,43,44)(H,45,46)/t18-,19-,20+,21+,22?,23?,24?,25?,26-,28?,32+,33+,34+,35-,36-/m0/s1
	$C_{36}H_{54}O_{12}$	678.3615	$C_{30}H_{46}O_6$	*O*-glucuronidation of aliphatic acid	InChI=1S/C36H54O12/c1-31(2)11-13-36(29(44)45)14-12-33(4)17(18(36)15-31)7-8-20-32(3)16-19(37)26(41)35(6,21(32)9-10-34(20,33)5)30(46)48-28-24(40)22(38)23(39)25(47-28)27(42)43/h7,18-26,28,37-41H,8-16H2,1-6H3,(H,42,43)(H,44,45)/t18-,19-,20+,21+,22?,23?,24?,25?,26-,28?,32+,33+,34+,35-,36-/m0/s1
	$C_{36}H_{54}O_{12}$	678.3615	$C_{30}H_{46}O_6$	*O*-glucuronidation of aliphatic acid	InChI=1S/C36H54O12/c1-31(2)11-13-36(30(46)48-28-24(40)22(38)23(39)25(47-28)27(42)43)14-12-33(4)17(18(36)15-31)7-8-20-32(3)16-19(37)26(41)35(6,29(44)45)21(32)9-10-34(20,33)5/h7,18-26,28,37-41H,8-16H2,1-6H3,(H,42,43)(H,44,45)/t18-,19-,20+,21+,22?,23?,24?,25?,26-,28?,32+,33+,34+,35-,36-/m0/s1
	$C_{30}H_{46}O_9S$	582.2862	$C_{30}H_{46}O_6$	Sulfation of secondary alcohol	InChI=1S/C30H46O9S/c1-25(2)11-13-30(24(34)35)14-12-27(4)17(18(30)15-25)7-8-20-26(3)16-19(39-40(36,37)38)22(31)29(6,23(32)33)21(26)9-10-28(20,27)5/h7,18-22,31H,8-16H2,1-6H3,(H,32,33)(H,34,35)(H,36,37,38)/t18-,19-,20+,21+,22-,26+,27+,28+,29-,30-/m0/s1
	$C_{30}H_{46}O_9S$	582.2862	$C_{30}H_{46}O_6$	Sulfation of secondary alcohol	InChI=1S/C30H46O9S/c1-25(2)11-13-30(24(34)35)14-12-27(4)17(18(30)15-25)7-8-20-26(3)16-19(31)22(40-41(36,37,38)39)29(6,23(32)33)21(26)9-10-28(20,27)5/h7,18-22,31H,8-16H2,1-6H3,(H,32,33)(H,34,35)(H,36,37,38)/t18-,19-,20+,21+,22-,26+,27+,28+,29-,30-/m0/s1

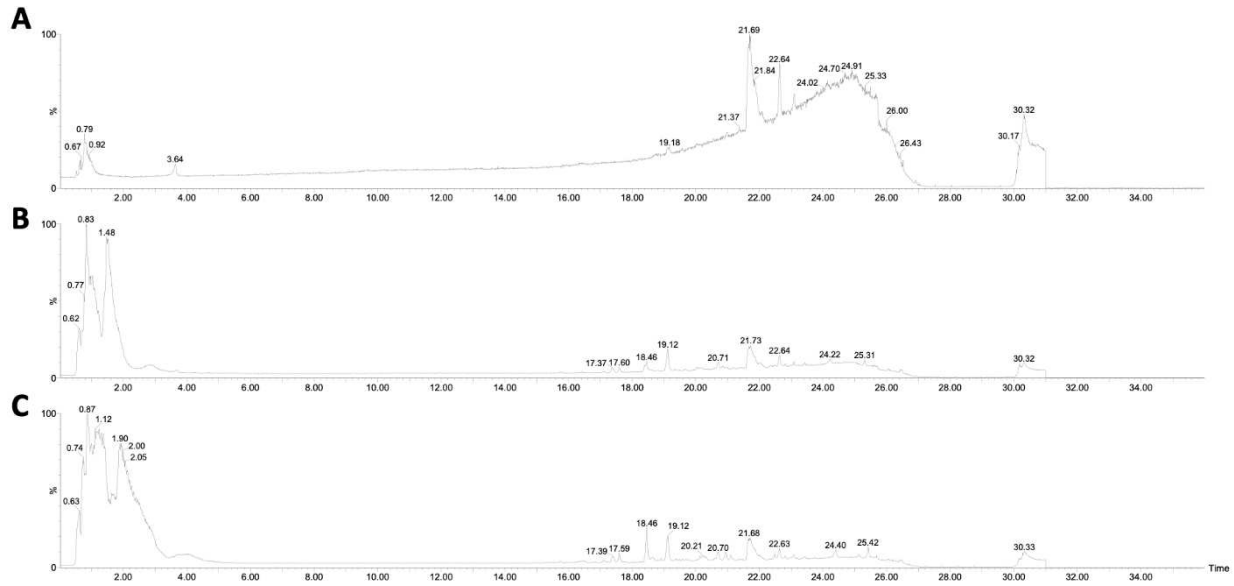

487

488 *Figure SI 1: TIC before (A), after 1h (B) and after 3h (C) S9 biotransformation*

489

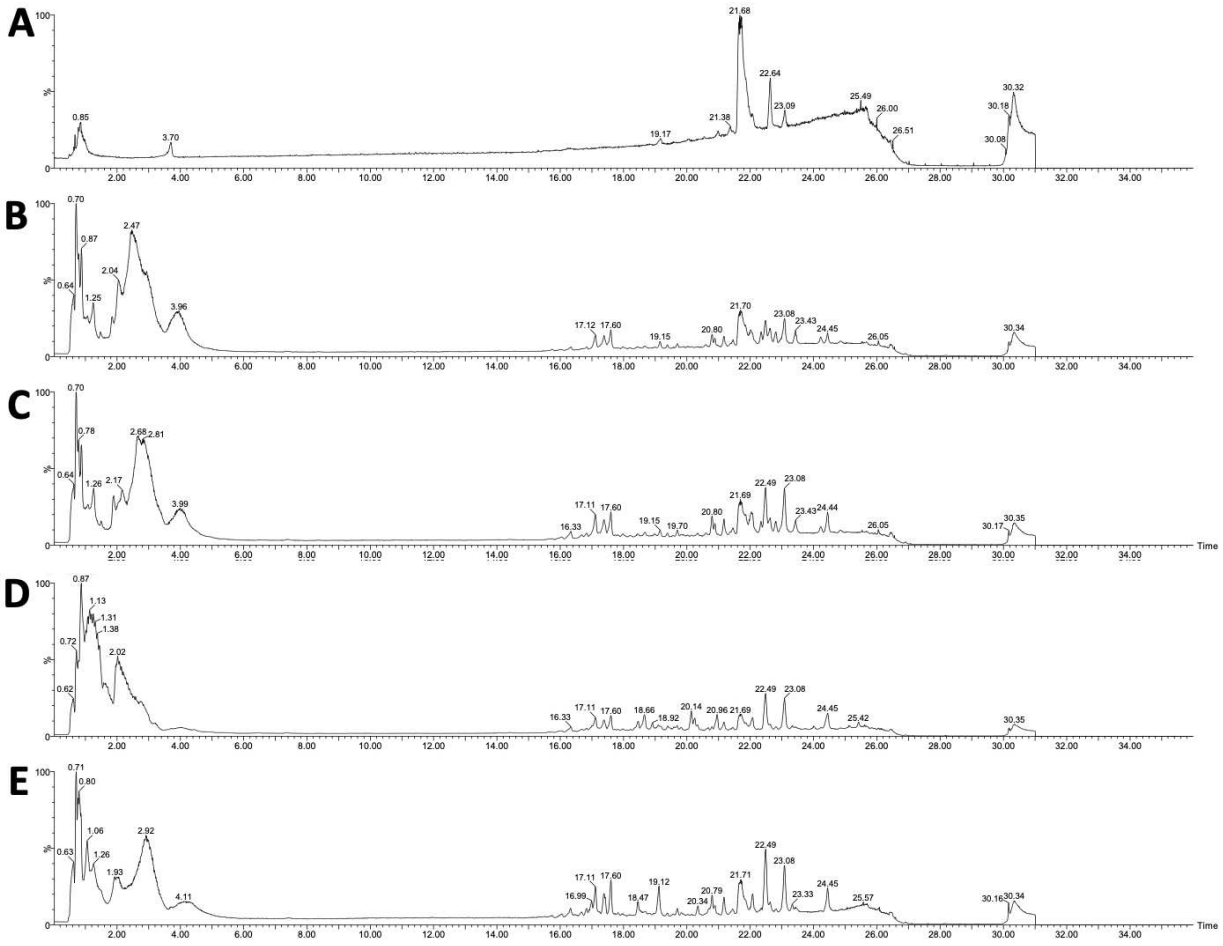

490

491 *Figure SI 2: TIC of HLM + HLCYT biotransformations: before (A), after 1h (B) and after 3h (C) of Phase I biotransformation,*
492 *after Phase II glucuronidation (D) and sulfation (E)*

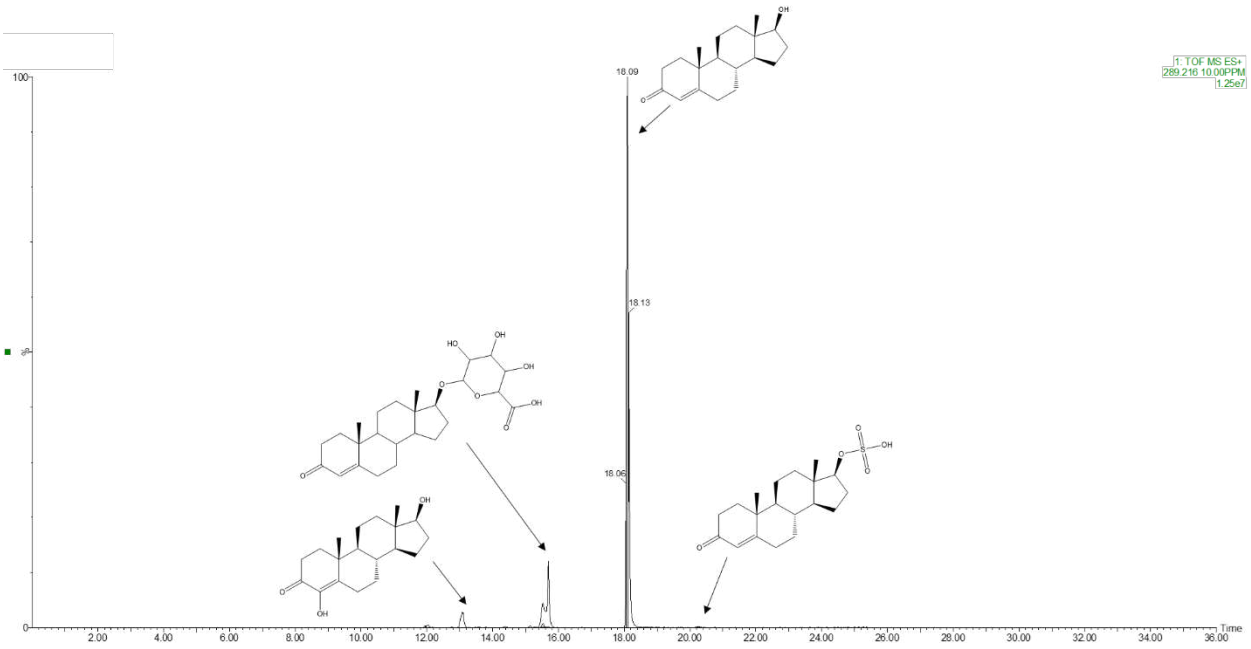

493

494 *Figure SI 3: Overlay of extracted ion chromatograms of testosterone and its metabolites after hepatic biotransformation*
495 *using S9.*

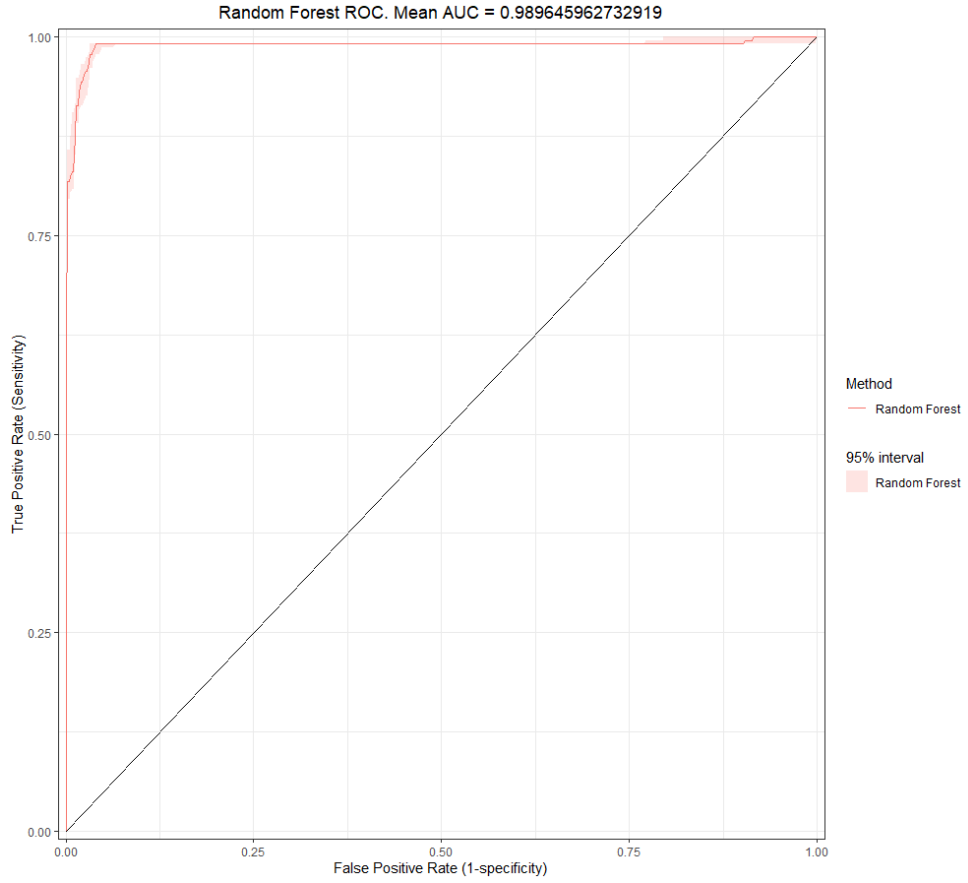

496

497 *Figure SI 4: ROC for the random forest model of biotransformation using S9*

498

499

500

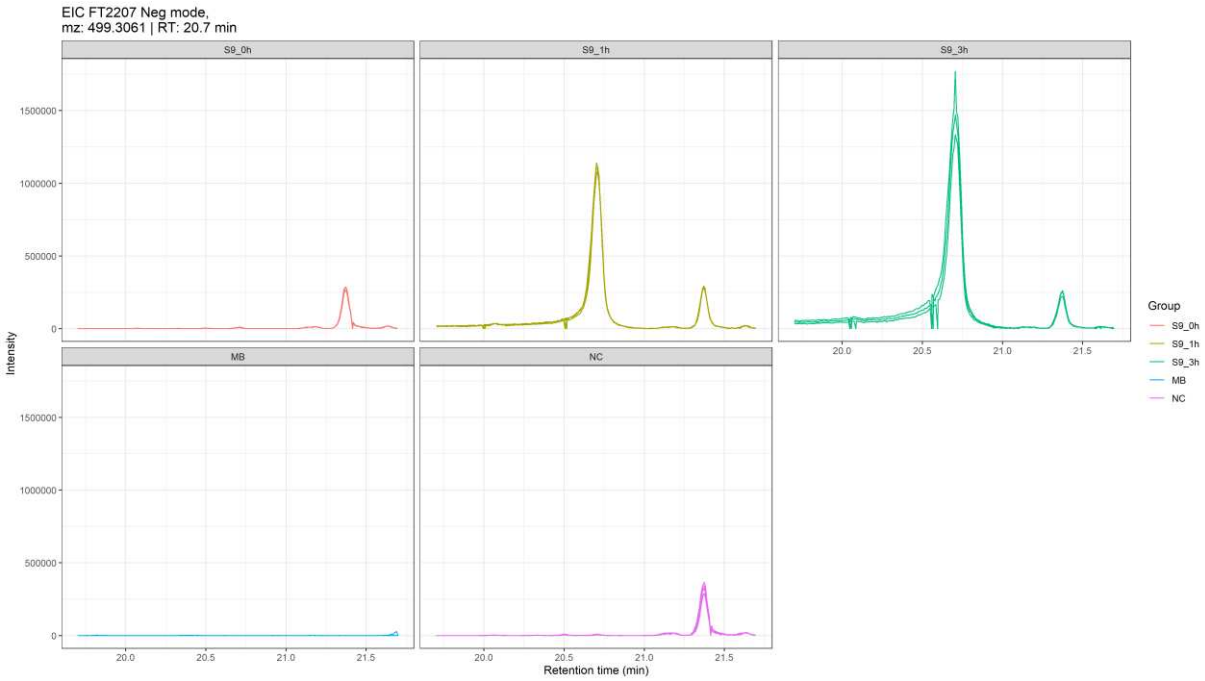

Figure SI 5: Example of facet plots (M5 - S9 biotransformation)

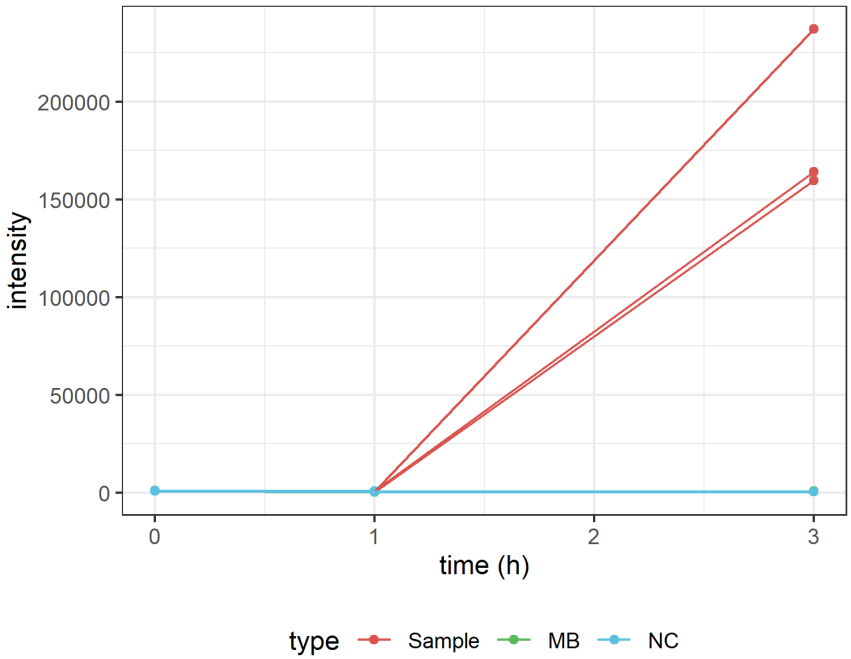

Figure SI 6: Time profile of the biotransformation for M11 using HLM + HLCYT in samples, negative controls (NC) and blank (MB).